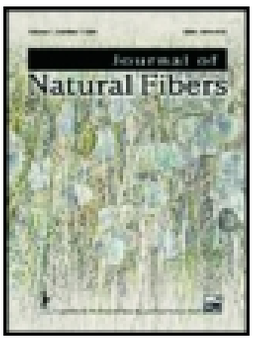

Journal of Natural Fibers

ISSN: (Print) (Online) Journal homepage: https://www.tandfonline.com/loi/wjnf20

Properties of Frost-Retted Hemp Fibers for the Reinforcement of Composites

Laetitia Marrot, Percy Festus Alao, Valdek Mikli & Jaan Kers

To cite this article: Laetitia Marrot, Percy Festus Alao, Valdek Mikli & Jaan Kers (2021): Properties of Frost-Retted Hemp Fibers for the Reinforcement of Composites, Journal of Natural Fibers, DOI: 10.1080/15440478.2021.1904474

To link to this article: https://doi.org/10.1080/15440478.2021.1904474

Published online: 17 Apr 2021.

JOURNAL OF NATURAL FIBERS
https://doi.org/10.1080/15440478.2021.1904474

Taylor & Francis
Taylor & Francis Group

ARTICLE

OPEN ACCESS Check for updates

Properties of Frost-Retted Hemp Fibers for the Reinforcement of Composites

Laetitia Marrot[1,2], Percy Festus Alao[3], Valdek Mikli[3], and Jaan Kers[3]

[1]Renewable Materials Composites Group, InnoRenew CoE, Izola, Slovenia; [2]University of Primorska, Koper, Slovenia; [3]Department of Polymer Materials, Tallinn University of Technology, Tallinn, Estonia

ABSTRACT

Frost-retted hemp fibers were investigated to assess their suitability for composite applications. Chemical analysis of frost-retted hemp fibers highlighted a high amount of solubles (pectins) at the fibers surface and a low lignin content in the fibers that was attributed to an unfavorable synthesis of lignin in the cell wall due to the particularly cold temperature during hemp growth in the Nordic countries. The fibers tensile properties were considered at two different scales and the performances of hemp/PLA composites were assessed. Recommendations were provided for the use of frost-retted hemp fibers in the reinforcement of thermoplastic composites.

摘要

研究了霜脱胶大麻纤维对复合材料的适用性. 对霜脱胶大麻纤维的化学分析表明, 纤维表面有大量的可溶物（果胶）, 纤维中的木质素含量较低, 这是由于北欧国家大麻生长期间温度特别低, 不利于细胞壁木质素的合成. 研究了纤维在两种不同尺度下的拉伸性能, 并对大麻/聚乳酸复合材料的性能进行了评价. 提出了霜麻纤维增强热塑性复合材料的建议.

KEYWORDS

Hemp; frost-retting; nordic country; tisza variety; PLA composite; polylactic acid composite

关键词

大麻; 霜冻脱胶; 北欧国家; 提萨品种; 复合材料; 聚乳酸复合材料

Introduction

Natural plant fibers as reinforcement of composites have received a growing interest from the scientific community for the last 15 years (Bourmaud et al. 2018). Industrial hemp (*Cannabis sativa*) is an annual crop that requires low input for its cultivation (Horne 2020), fitting into sustainable farming systems (Ranalli and Venturi 2004). In Nordic countries, hemp is primarily cultivated to produce cannabidiol for medicine application. Flowers and leaves are harvested in September while the straws (including fibers and shives) are considered as a waste or low-value product. Hemp fibers are extracted from the straws through a mechanical defibration process that crushes the stems. Prior to the decortication, the straws can undergo a retting process (1) to loosen bonding between fiber-fiber and bundle-bundle by degrading the non-cellulosic components in the bast fiber layer, particularly the pectic polysaccharides (Horne 2020); and (2) to facilitate fiber separation and to avoid fiber breakage during following mechanical processing (e.g. scutching) and to preserve the fibers quality (Gregoire et al. 2019). Western European field retting consists of leaving purposefully the stems in the field after the autumn harvest to be decorticated under the actions of microorganisms. The time of field retting depends on the geographic location and weather conditions. In Nordic countries, autumn is a cold and rainy period. If harvested at that time, due to the high moisture content, hemp stems require a high amount of energy to dry and avoid the formation of mold that could destroy the quality of the raw material (Pasila 2000). Pasila (Pasila 2000) suggested harvesting the straw in spring, which is the driest time of the year. Hemp straws harvested in spring are defined as "frost-retted". Under frost-retting, the

CONTACT Laetitia Marrot laetitia.marrot@innorenew.eu Renewable Materials Composites Group, InnoRenew CoE, Livade 6, Izola 6310, Slovenia.

fiber separation from the stem is induced by the daily changes of temperature above and below the zero in the springtime. The water freezes and melts in the plant cell structures, which leads to an enlarging movement that loosens the bast fiber from the stem (Pasila 2000). The main goal of this paper is to assess the suitability of frost-retted hemp fibers for composite applications in order to value this by-product of the Nordic hemp industry. The study will present the chemical composition and the mechanical properties of hemp fibers (*Cannabis sativa*, dioecious Hungarian variety Tisza) that underwent a frost-retting process, and the mechanical performances of Polylactic acid (PLA) composites using these frost-retted fibers as reinforcement. This study will provide data on the Tisza variety, which is not often reported in the literature. The mechanical analysis of the frost-retted hemp fibers will be performed for two scales of reinforcement (unitary fibers and strands), and the performances of the corresponding PLA composites will be investigated to provide good practices for the manufacture of sustainable composites using frost-retted fibers.

Materials and methods

Materials

Hemp fibers (*Cannabis sativa*, dioecious Hungarian variety Tisza) were supplied by Hempson OÜ. They were sown the 10 June 2016 in Estonia on the Saaremaa island. Growth lasted until October 2016, and, after senescence, the stems stood in the field until 4 May 2017 before being harvested. Between June and October 2016, the average monthly temperatures were 15, 18, 17, 15 and 7°C, and the average monthly light were 13.0, 11.5, 8.9, 8.6, 4.0 hours/day. During the frost-retting period (November 2016 – May 2017), the average monthly temperatures were 3, 3, 0, 0, 2, 4, 9°C. The stems were then industrially decorticated by a mechanical process.

PLA fibers (Ingeo™) from Trevira® GmbH were used for the manufacture of composites. The fibers were 60 mm long, with a round cross-section, a finesse of 6.7 dtex, and a density of 1.25 g/cm^3.

Microscopic analysis of hemp fibers

Fibers surface and individualization were observed with a high-resolution Zeiss Ultra 55 Scanning Electron Microscope (SEM). Prior to the observation, the fibers were vacuum coated with an alloy of gold/palladium (80/20). The machine was operated between 4 and 20 kV, scanning depth up to 100 nm, and magnification up to 50000.

The individualization of the fibers was quantified by image analysis. The fibers were first embedded in epoxy resin, then the cross-section of the sample was polished and observed with a digital microscope Keyence VHX-6000. The images were analyzed with the ImageJ software. The type was converted into 8-bit, a threshold was applied, and the image was processed to reduce noise and fill the holes before analyzing the particles. The particle analysis provided surface areas of 671 fibers and bundles units, and corresponding equivalent diameters of these units were estimated by considering a circular shape for their cross-section.

Chemical analysis of hemp fibers

Chemical composition of the untreated hemp batch was determined by the Van Soest method, based on standards NF EN ISO 13906 and NF V18-122. This method uses a successive and differential solubilization of the constituents of the samples (constituents of the plant cell walls mainly) in 3 detergents followed by a calcination. The Neutral Detergent Fiber (NDF) attack ensures a partial removal of pectins. NDF composition is 30 g/L of sodium dodecyl sulfate, 18.61 g/L of ethylenediaminetetraacetic acid (EDTA), 6.81 g/L of sodium borate, and 4.56 g/L of disodium hydrogenophosphate dihydrate. The Acid Detergent Fiber (ADF) attack then eliminates pectins and hemicelluloses. ADF is made of 20 g/L of cetyl trimethylammonium bromide in H_2SO_4 at 0.5 mol/L. Each extraction

lasts for 1 h at 100°C and is followed by 2 rinsing steps for 1 h with boiling water. The Acid Detergent Lignin (ADL) attack on ADF residues consists of an acidic solution of 72% H_2SO_4 (12 mol/L) and allows the elimination of cellulose. The last calcination step eliminates lignin in ADL residues. Monitoring the mass of the samples during these successive specific attacks makes it possible to obtain sequentially the cellulose content, an estimate of the hemicelluloses content, an estimate of the soluble content (part of pectins), the lignin content, and the ash content (inorganic matter). In practice, the chemical analysis of the hemp fibers was performed with FIBRETHERM® equipment (Gerhardt) including a control sample and allowed accurate result with a precision of 0.1% for the components content. The chemical composition corresponds to the average and standard deviation of duplicates.

Composite preparation and evaluation of fibers orientation

Hemp fibers and PLA fibers were dried in an oven for 24 hours at a temperature of 80°C prior to the composite preparation. Two ratios hemp fibers/PLA (30 and 50 wt% regarding hemp fibers weight) were prepared. Hemp and PLA fibers were weighed using a Mettler Toledo PL202-s and then combined using a drum carder of 100 mm width. Aligned hemp and PLA fibers were then mixed and placed in a metal mold of dimensions 300 × 300 x 4 mm. The mixture was compressed for 10 min at a temperature of 180°C and a pressure of 3 MPa. Finally, the composite product was conditioned at room temperature (23°C) before removal from the form.

Within the composites, the fibers are unidirectionally aligned, but, given their inhomogeneity in terms of dimensions and their entanglement, there is a clear misalignment that needs to be taken into account. For this purpose, surface analysis on the longitudinal section of the composites was operated under a digital microscope Keyence VHX-6000. Considering that the average misalignment is the same within the thickness of the composites, the misorientation of the fibers and strands in regard to the loading direction was measured. A total of 105 angle measurements were taken on the samples machined for tensile tests.

Mechanical characterization of fibers and composites

Natural fibers can be mechanically characterized either at the unitary fiber scale or at the bundle of fibers (strands) scale. Dispersion of the mechanical properties of hemp and flax unitary fibers has been discussed in the literature (Lefeuvre et al. 2014; Marrot et al. 2013). To reduce variability, Barbulée et Gomina (Barbulée and Gomina 2017) suggest testing strands that gather hundreds of unitary fibers. They obtain a convergence of the average deformation with about 1% accuracy when testing 15 strands (Barbulée and Gomina 2017). In this study, the mechanical properties of the fibrous reinforcement were tested at two scales (unitary fiber and strand) to consider the influence of the fiber dimensions on the reported values and dispersion. Tensile tests on unitary hemp fibers and strands were carried out on a universal testing machine Zwick Roell Z010 at 23 ± 1°C and 50 ± 2% RH. The tensile test on unitary fibers has been carried out in accordance with the NF T25-501-3 standard describing the determination of tensile properties of flax unitary fibers for application in the reinforcement of plastic composites. To the best of the authors knowledge, there is no equivalent standard for the mechanical characterization of hemp fibers. The machine was equipped with a 20 N load cell, gauge length was taken at 10 mm, deformation was obtained using cross-head travel, and strain rate was set at 1 mm/min. Before testing, the mean diameter was determined as the average of 3 diameter measurements. A total of 64 unitary fibers were tested among which 19 were not exploitable (break in the jaws). For the tensile test on strands, the machine was equipped with a 10 kN load cell, gauge length was fixed at 50 mm, and strain rate was set at 1 mm/min. The choice of the gauge length resulted in taking the maximal length allowing homogeneous fineness along the whole length of the strand. 42 strands were tested (1 sample was not exploitable). Prior to the test, the mass of the strands with a length of 10 cm was measured with a Mettler Toledo XPR303S scale (1 mg precision), and the corresponding average

diameter of the strands was calculated by using the density of the hemp fibers estimated by Bourmaud et al (Bourmaud et al. 2019) at 1,38 g/cm^3 with the buoyancy method.

Five composite samples were tested following EN–ISO 527–4 using an INSTRON 5688 tensile machine. The test condition was at a temperature of 24°C, relative humidity of 40%, and test rate of 2 mm/min. The specimens were conditioned in the room for 24 h before the test, and the test results were averaged arithmetically.

Fiber massic fraction (M_f %) was determined as the weight of the fibrous reinforcement (W_f) divided by the total weight of the composite ($W_f + W_m + W_p$), f, m and p indexes standing, respectively, for fiber, matrix and porosity. Since the weight of the voids Wp is taken as 0:

$$M_f\% = \frac{W_f}{W_f + W_m + W_p} = \frac{W_f}{W_f + W_m}$$

The fiber volume fraction (V_f %) is given by the relation:

$$V_f\% = \frac{M_f\%}{M_f\% + \left(\frac{\rho_f}{\rho_m}\right)\left(1 - M_f\%\right)}$$

With ρ_f as the density of fibrous reinforcement (1.38 according to (Bourmaud et al. 2019) as mentioned above) and ρ_m as the density of the PLA matrix (1.25 according to the FDS).

Composites density (ρ_c) was calculated using the weight and volume of the samples. The void fraction (V_p%) was then calculated from the measured weights and densities:

$$V_p\% = 1 - \frac{\frac{W_f}{\rho_f} + \frac{W_c - W_f}{\rho_m}}{\frac{W_c}{\rho_c}}$$

Results and discussion

Investigation of biochemical composition

Chemical composition of the frost-retted hemp fibers is presented in Table 1. Cellulose content (77.4 ± 0.3% w/w) is in accordance with results from the literature (Liu et al. 2015; Marrot et al. 2013). Pectins content is related to the soluble content extracted by the Van Soest method. In this study, the soluble content (12.6 ± 0.4% w/w) is relatively high compared to values from the literature. Marrot et al (Marrot et al. 2013) reported a pectins content of 3.0% w/w. Liu et al (Liu et al. 2015) noted a reduction of the pectin deposition (indicated by galacturonic acid content) from 6.3 for un-retted fibers to 3.1–5.4% w/w for field-retted fibers. However, in the case of frost-retting, the separation of the fibers from the stem is due to the variation of volume of alternatively liquid and solid water in the cell plant structure under the effect of negative temperatures. Under such low temperature conditions, the activity of microorganisms and enzymes is limited, and the pectic substances are less prone to degradation than in the case of dew-retting. Lignin content in this study (1.4% w/w) is particularly low compared with values reported in the literature (between 2 and 6% of dry matter (Angelini, Tavarini, and Di Candilo 2016; Müssig et al. 2020)). The phenological development of hemp is conditioned by climatic conditions, in particular to light and temperature (Hall, Bhattarai, and Midmore 2014). As lignin is a component which is biosynthesized in the final stage of the fiber-cell wall remodeling (Crônier, Monties, and Chabbert 2005), the relatively cold temperature and short

Table 1. Chemical composition of the frost-retted hemp fibers.

Cellulose (%)	Hemicellulose (%)	Lignin (%)	Soluble (%)	Inorganic matter (%)
77.4 ± 0.3	8.3 ± 0.3	1.4 ± 0.0	12.6 ± 0.4	0.3 ± 0.0

daily light period at this stage in Estonia may be responsible for an unfavorable synthesis of lignin in the cell wall, resulting in a lower content as the one usually reported for Western European hemp varieties. Similarly, authors (Gindl, Grabner, and Wimmer 2000) reported the influence of climatic variability on the lignification of the cell wall in latewood of Norway spruce.

Hemp fibers individualization

SEM observations of the frost-retted hemp fibers highlighted the presence of large bundles, up to 300 µm in diameter, mixed with unitary fibers (Figure 1A). Significant amounts of impurities (cortical residues, pectins, and wax) were observed on the bundles surface (Figure 1B), preventing their further individualization. This observation is in good agreement with the high soluble content highlighted by the chemical analysis of the fibers.

The image analysis of the cross-section of the fibers highlighted a broad repartition of fiber equivalent diameters from 11 µm to 525 µm. The number of fiber or bundle units per equivalent diameter range is presented on the Figure 2. Unitary fibers (with equivalent diameter in the range 11–30 µm) represent 12.5% of the total number, and 0.5% of the total surface area of the fibrous units. Small bundles (with equivalent diameter in the range 31–110 µm) represent 49.6% of the total number, and 11.7% of the total surface area of the fibrous units. Large bundles (with equivalent diameter higher than 111 µm) represent 37.9% of the total number, and 87.8% of the total surface area of the fibrous units.

Tensile mechanical properties of unitary fibers and strands

The force–deformation curves of a unitary fiber and a strand under tension are presented, respectively, in Figures 3 and 4. In the case of loading for a unitary fiber, the non-linear region observed in the beginning of the curve is typical to plant fibers and corresponds to the alignment of the microfibrils with the fiber axis (Baley 2002; Marrot et al. 2013). The apparent modulus of the unitary fiber is taken in the second region of the loading curve, which is linear and characteristic of an elastic behavior (Figure 3).

In the case of loading for a strand (Figure 4), one or several bundles of fibers are solicited.

Two types of rupture are observed (Figure 4). The first one is a brittle fracture of the strand; the constitutive fibers are linked strongly enough by the pectic interphase to be loaded simultaneously, which results in a single linear region on the loading curve where the apparent modulus is taken. When maximal load is reached, the fibers show a simultaneous brittle fracture. For the second type of rupture, once the bundles reach an equal strain, the loading curve displays a first linear region that corresponds to an elastic behavior. The apparent modulus is measured in this elastic domain (Figure 4). Then the curve shows a non-linear zone ending by the first breakdown of a fiber bundle. The load is then carried by the remaining bundles until the failure of another fiber bundle, and so on. until the break of the last bundle. This succession of breaks and load recovery gives a typical saw-tooth shape to the loading curve, previously described by Barbulée et al (Barbulée et al. 2014) for tension of flax slivers. These authors (Barbulée et al. 2014) observed three types of damage mechanisms in the non-linear zone thanks to acoustic emission analysis: first bundles delamination by breakage of the pectin links between ultimate fibers, then delamination among adjacent bundles, and finally successive ruptures of the bundles occur (Barbulée et al. 2014). The two types of fracture highlight the heterogeneity of the frost-retted strands, which gather bundles strongly connected to each other and bundles with poor cohesion due to degradation of the middle lamellae during the retting process.

In Figure 5, strength at break is plotted versus apparent modulus for unitary fibers and bundles of frost-retted hemp fibers tested in this study. The linear tendency reported in the literature (Bourmaud et al. 2018; Marrot et al. 2013) for this plot is visible for the unitary fibers, with a determination coefficient r^2 at 0.61. For the strands, the linear tendency is not confirmed ($r^2 = 0.06$). Unlike unitary

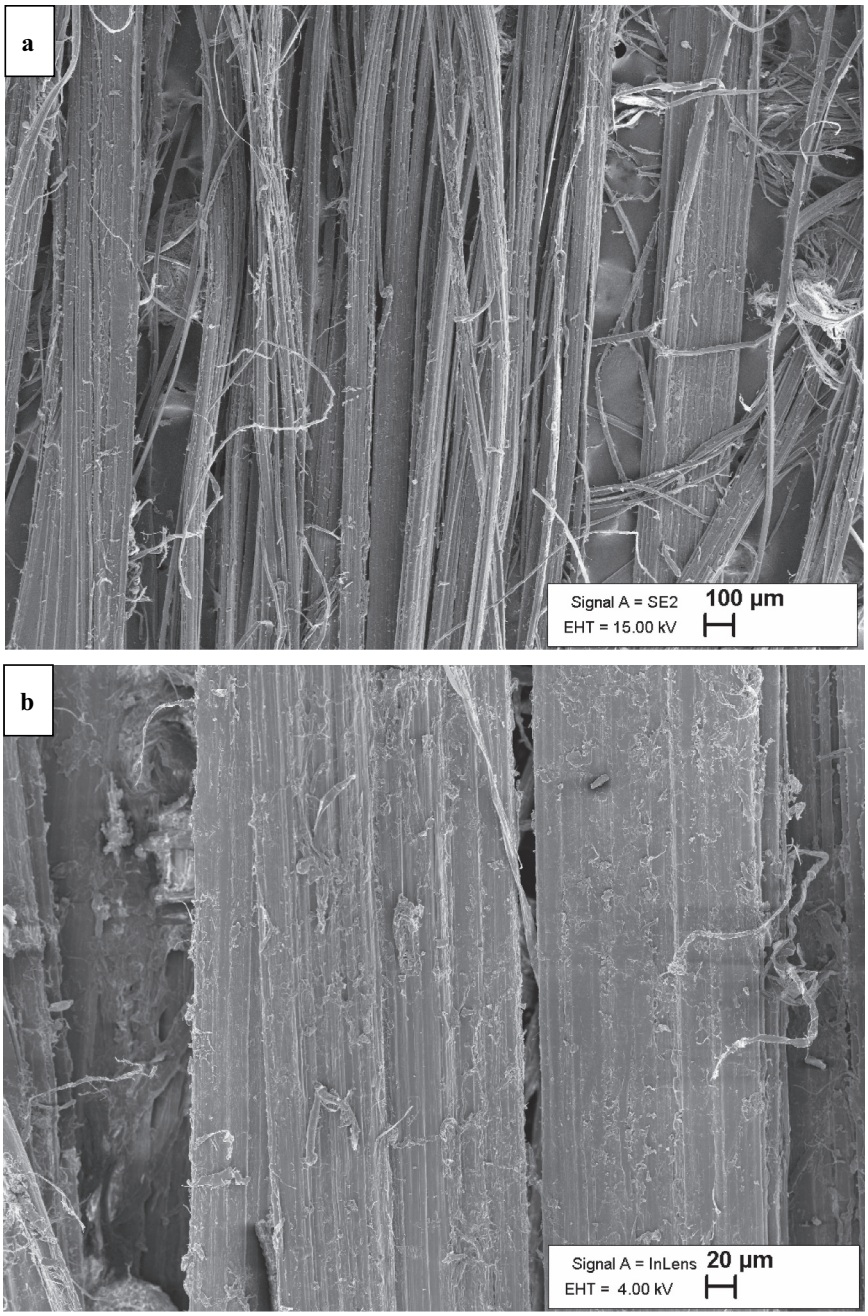

Figure 1. SEM observation of the frost retted hemp fibers: a) Presence of large bundles of fibers mixed with single fibers b) Cortical residues on the hemp fibers surface.

fibers, strands are heterogeneous materials where several types of damages occur during breakage, which explains why apparent modulus and strength at break are not strongly correlated.

The average tensile properties of the two materials are presented in Table 2.

Regarding unitary fibers, in spite of their high cellulose content observed during the chemical composition analysis in the section 5.1, the average value for apparent modulus (16.6 ± 8.5 GPa) is in the lower range of the data from the literature (14.4–51 GPa (Bourmaud et al. 2018; Gregoire et al.

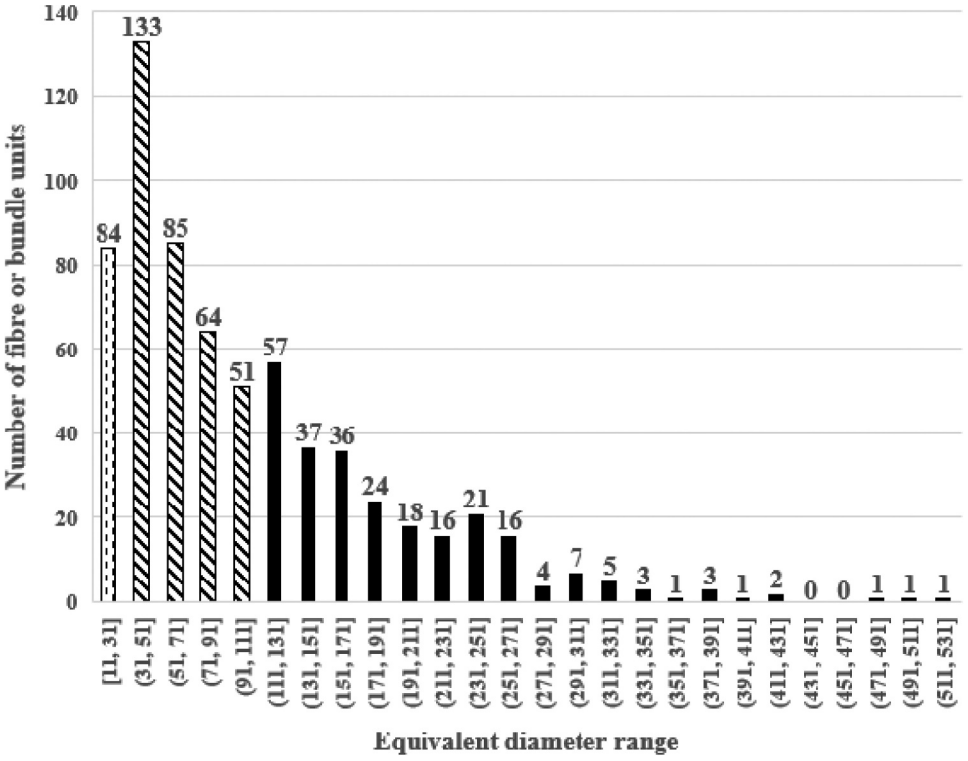

Figure 2. Number of fiber or bundle units per equivalent diameter range.

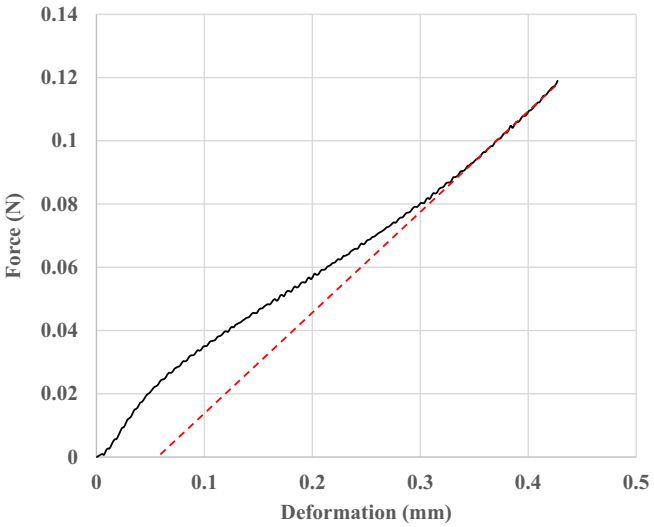

Figure 3. Force-deformation curves of a single fiber.

2019)), and the average value for the strength (500 ± 239 MPa) is in the middle range of the data available in the literature (285–969 MPa) (Bourmaud et al. 2018). The relatively low mechanical properties might be related to the low lignin content measured in our fibers from the Tisza variety compared to the values usually reported for Western European hemp varieties. Indeed, Liu et al (Liu

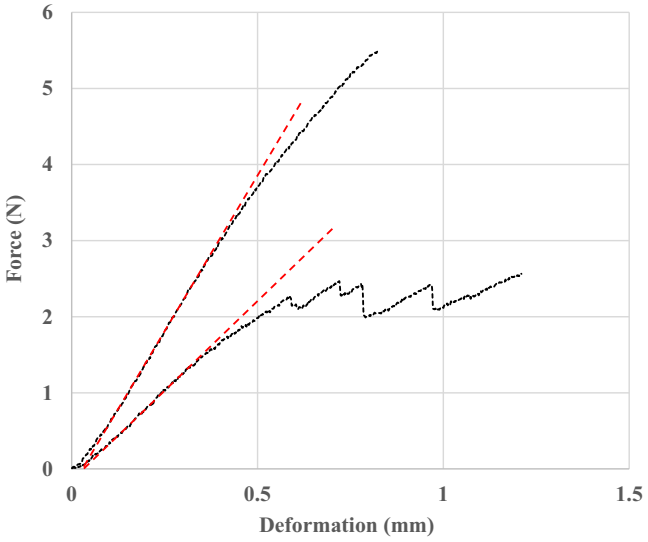

Figure 4. Force-deformation curves of strands under tension.

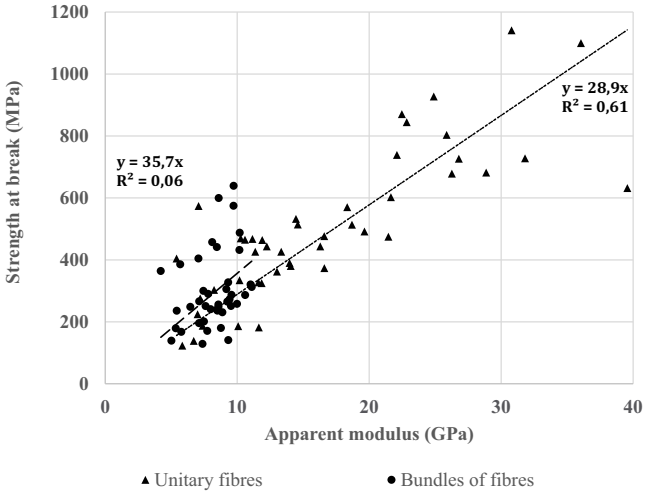

Figure 5. Tensile properties of frost retted hemp unitary fibers and strands.

Table 2. Average tensile properties of unitary fibers and strands of frost-retted hemp fibers.

Material	Number	Diameter (µm)	Modulus (GPa)	Strength (MPa)	Strain at break (%)
Unitary fibers	45	18 ± 5	16.6 ± 8.5	500 ± 239	2.9 ± 1.0
Strands	41	190 ± 64	8.2 ± 1.7	298 ± 123	1.9 ± 0.9

et al. 2017) showed the important role of lignin polymerization in the increase of the mechanical properties of their fibers.

The tensile test of the strands results in lower mechanical properties than the ones measured on unitary fibers: average apparent modulus is 8.2 ± 1.7 GPa and average tensile strength is 298 ± 123 MPa. Different composition and size of the tested materials might have contributed to this result. First, the length of a unitary fiber was found to be around 15 mm during their extraction from the strands prior to the tensile test. The gauge length for the tensile test is taken at 10 mm, i.e. shorter than the

length of a unitary fiber so there likely is only one unitary fiber tested between the clamps. Since the gauge length is fixed at 50 mm for the strands (so roughly 3 times the unitary fiber length) and the average diameter of the strands is found to be slightly higher than 10 times the average diameter of the unitary fibers (see Table 2), a strand gathers at least 300 unitary fibers. The middle lamella, pectin interphase between unitary fibers, is a critical area where failure may happen under tension load (Bos, Van Den Oever, and Peters 2002). The strands tensile properties are then dictated by both unitary fibers and middle lamella resistances. The contribution of the middle lamella in the flax bundle strength has previously been highlighted by Charlet et Beakou (Karine Charlet and Béakou 2011); the authors observed a decrease of the tensile strength while increasing the sample gauge length above the length of the elementary fibers. In this study, we fixed the gauge length at 50 mm to ensure a homogeneity of the fineness along the length of the strand. Nevertheless, for longer gauge lengths, the strength at break would likely decrease, as depicted in the literature (Romhány, Karger-Kocsis, and Czigány 2003), for the reasons described above. Réquilé et al (Réquilé et al. 2018) measured the tensile mechanical properties of hemp fiber-rich outer-tissues including epidermis, fiber bundles, and phloem. With the same gauge length of 50 mm and despite the presence of epidermis and cortical parenchyma in addition to the bundles, the authors (Réquilé et al. 2018) obtained performances in the same range as the ones presented in this study (10.27 ± 1.83 GPa for the apparent modulus and 172.4 ± 76.7 MPa for the tensile strength of dew-retted hemp fiber-rich outer tissues).

Moreover, due to averaging effect of the important number of fibers within a strand, the standard deviation is lower in the case of strands compared with unitary fibers. The dispersion is particularly reduced for the apparent modulus (20% for strands and 51% for unitary fibers, respectively) and, to a lower extent, for the tensile strength (41% and 47%, respectively). The dispersion is clearly visible on the curves of apparent modulus (Figure 6) and tensile strength at break (Figure 7) plotted versus the equivalent diameter of the fibrous unit (unitary fibers and strands together). Both variables decrease when the equivalent diameter increase. For unitary fibers, the decrease of tensile strength at break with increasing diameter is due to the increasing probability of having a flaw in the fiber. This phenomena was first highlighted by Griffith in the frame of the rupture mechanics of fragile materials (Griffith and Taylor 1921) and the weakest link model describes statistically the higher chances of finding a critical flaw when increasing the diameter of the fiber. The decrease of apparent modulus with the diameter of the unitary fibers is attributed to an overestimation of effective cross-section due to the presence of the lumen (void) in the fiber which is not considered. At the bundle

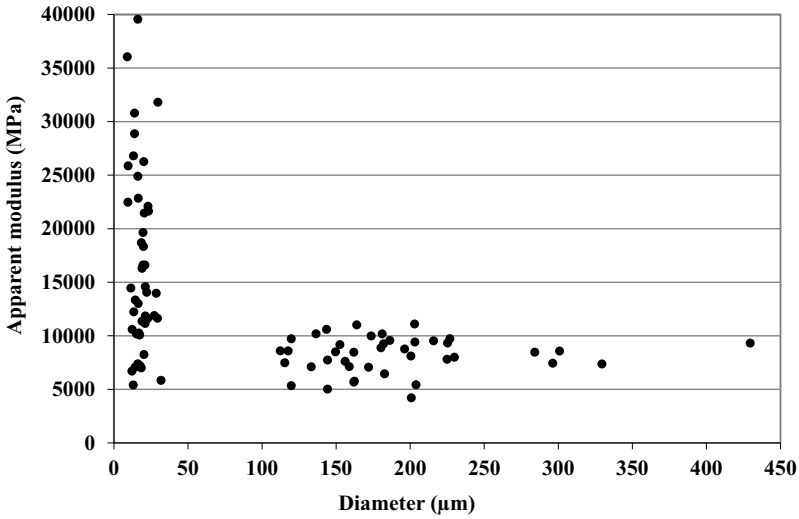

Figure 6. Apparent modulus depending on the diameter of the fibrous unit (unitary fiber or strand).

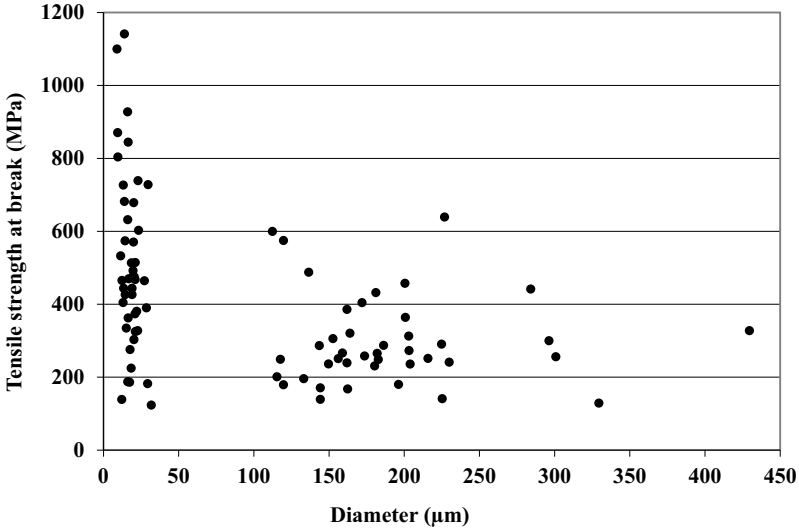

Figure 7. Tensile strength at break depending on the diameter of the fibrous unit (unitary fiber or strand).

scale, the decrease of both variables with diameter is due to the combined types of damages occurring during breakage, as described above.

Properties of aligned hemp/PLA composites

Under a unidirectional tensile load, an optimum reinforcement is achieved when the fibers are perfectly aligned, individualized (Coroller et al. 2013; Marrot et al. 2014), and homogeneously distributed in the matrix. In this study, the average misalignment of the fibers regarding the load direction was estimated at 25° by image analysis. Additionally, we detailed the level of hemp fibers individualization in section 2. We observed that the fibrous reinforcement is mainly constituted of small and large bundles of fibers (99.5% of the total surface area of the fibers cross-section), and we highlighted in section 5.3 the different performances at the unitary fiber scale and the strands scale and provided average mechanical properties for both types of reinforcement. Under these conditions, the mechanical properties of hemp/PLA composites with 30 and 50 wt% of hemp fibers were investigated by tensile tests. Table 3 gathers the experimental average tensile mechanical properties measured for the hemp/PLA composites. The Young modulus of the composites with 30 wt% and 50 wt% is, respectively, 79 and 149% higher than the modulus of the unreinforced PLA (2.7 GPa). This significant increase can be attributed to the higher modulus of the fibers compared to PLA and shows that the Young modulus of the composites is mainly governed by the fiber content and less dependent on the fiber/matrix interface. The strength at break of the composites was increased by 12% with 30 wt% fibers but decreased by 40% with 50 wt% fibers (strength at break of the unreinforced PLA was found to be 46 MPa). In the first case, with 30 wt% reinforcement, the standard deviation is quite high (18%) suggesting poor uniformity of fiber distribution throughout the composite and fiber agglomeration. In the case of 50 wt% fibers, the standard deviation is smaller (9%), and the decrease in strength can be attributed to insufficient wetting of the fibers by the matrix and limited load transfer between the fibers

Table 3. Average tensile mechanical properties of hemp/PLA composites with 30 and 50% of hemp fibers by weight.

M_f (%wt)	V_f (%vol)	ρ_c (g/cm^3)	V_p (%)	ε_c (%)	$\sigma_{c,exp}$ (MPa)	$E_{c,exp}$ (GPa)
30	28	1.26	7	2.2 ± 0.5	51 ± 9	4.8 ± 0.3
50	48	1.04	17	2.6 ± 0.5	27 ± 3	6.7 ± 0.6

and matrix. The high amount of impurities highlighted by the microscopical observations and confirmed by the level of insolubles by chemical analysis prevents a good adhesion between fibers and matrix and is a weak point in the interface. The void fraction is estimated at 7% in the case of the composite reinforced by 30 wt% of hemp fibers and at 17% for the composites reinforced by 50 wt% of hemp fibers. The high void fraction observed at 50 wt% is due to the difficult wetting of the fibers during manufacturing. Poor wetting in non-woven hemp/PLA composites has been reported by Pickering et Aruan Efendy (Pickering and Aruan Efendy 2016) for fiber fraction higher than 30 wt %. It is commonly observed in the literature that the higher the volume fraction of fibers in composites, the higher the fraction of porosities, leading to an inherent reduction in mechanical properties (Madsen, Hoffmeyer, and Lilholt 2007). A way of improving the wetting of the fibers is to reduce the viscosity of the matrix during processing (Pickering and Aruan Efendy 2016). Following the analysis of the composite performances, the authors recommend to improve stress transfer in several ways: 1) avoiding agglomeration of fibers by using fibrous reinforcement that is more individualized, 2) limiting the creation of voids during the manufacturing process by improving the wetting of the fibers and using matrix with adequate viscosity, 3) improving the fiber/matrix adhesion by cleaning the fiber surface to limit the presence of impurities.

Conclusions

The mechanical properties of frost-retted hemp fibers were investigated to assess their suitability for composite applications. Chemical analysis of frost-retted hemp fibers highlighted a high amount of solubles (pectins) at the fibers surface and a low lignin content in the fibers that was attributed to an unfavorable synthesis of lignin in the cell wall due to the particularly cold temperature at this stage of hemp growth in Estonia. Tensile properties measured at two different scales showed values in the lower range of data available in the literature for unitary fibers and values comparable to the literature at the strands scale, and displaying a reduced standard deviation in the case of strands compared with unitary fibers. Hemp/PLA composites were manufactured by thermocompression with 30 and 50 wt% of fibers. Compared to the unreinforced matrix performances, composites' Young moduli were significantly improved by the addition of fibers. However, composites manufactured with 50 wt% of fibers displayed a high level of porosities that greatly impacted their tensile strength. In order to use frost-retted hemp fibers for composite applications, the authors recommend to preprocess the fibers to achieve a better individualization and clean their surface. For non-structural applications, using frost-retted hemp fibers for the reinforcement of thermoplastic composites is a good way to value this by-product of the Nordic hemp industry.

Acknowledgments

This work was supported by the Horizon 2020 Framework Program of the European Union; H2020 WIDESPREAD-2-Teaming [grant number 739574] and investment from the Republic of Slovenia and the European Regional Development Fund.

ORCID

Laetitia Marrot http://orcid.org/0000-0002-4244-2726
Percy Festus Alao http://orcid.org/0000-0002-9720-7037

Declaration of interest statement

The authors declare that they have no known competing financial interests or personal relationships that could have appeared to influence the work reported in this paper.

References

Angelini, L. G., S. Tavarini, and M. Di Candilo. 2016. Performance of new and traditional fiber hemp (Cannabis sativa L.) cultivars for novel applications: Stem, bark, and core yield and chemical composition. *Journal of Natural Fibers* 13 (2):238–52. doi:10.1080/15440478.2015.1029193.

Baley, C.. 2002. Analysis of the flax fibres tensile behaviour and analysis of the tensile stiffness increase. *Composites. Part A, Applied Science and Manufacturing* 33 (7):939–48. doi:10.1016/S1359-835X(02)00040-4.

Barbulée, A., and M. Gomina. 2017. Variability of the mechanical properties among flax fiber bundles and strands. *Procedia Engineering* 200:487–93. doi:10.1016/j.proeng.2017.07.068.

Barbulée, A., J.-P. Jernot, J. Bréard, and M. Gomina. 2014. Damage to flax fibre slivers under monotonic uniaxial tensile loading. *Composites. Part A, Applied Science and Manufacturing* 64:107–14. doi:10.1016/j.compositesa.2014.04.024.

Bos, H. L., M. J. A. Van Den Oever, and O. C. J. J. Peters. 2002. Tensile and compressive properties of flax fibers for natural fiber reinforced composites. *Journal of Materials Science* 37 (8):1683–92. doi:10.1023/A:1014925621252.

Bourmaud, A., J. Beaugrand, D. U. Shah, V. Placet, and C. Baley. 2018. Towards the design of high-performance plant fiber composites. *Progress in Materials Science* 97:347–408.

Bourmaud, A., J. Merotte, D. Siniscalco, M. Le Gall, V. Gager, A. Le Duigou, F. Pierre, Behlouli, K., Arnould, O., Beaugrand, J. et al.. 2019. Main criteria of sustainable natural fiber for efficient unidirectional biocomposites. *Composites. Part A, Applied Science and Manufacturing* 124:105504.

Charlet, K., and A. Béakou. 2011. Mechanical properties of interfaces within a flax bundle – part I: Experimental analysis. *International Journal of Adhesion and Adhesives* 31 (8):875–81.

Coroller, G., A. Lefeuvre, A. Le Duigou, A. Bourmaud, G. Ausias, T. Gaudry, and C. Baley. 2013. Effect of flax fibers individualisation on tensile failure of flax/epoxy unidirectional composite. *Composites. Part A, Applied Science and Manufacturing* 51:62–70.

Crônier, D., B. Monties, and B. Chabbert. 2005. Structure and chemical composition of bast fibers isolated from developing hemp stem. *Journal of Agricultural and Food Chemistry* 53 (21):8279–89.

Gindl, W., M. Grabner, and R. Wimmer. 2000. The influence of temperature on latewood lignin content in treeline norway spruce compared with maximum density and ring width. *Trees* 14 (7):409–14.

Gregoire, M., E. De Luycker, M. Bar, S. Musio, S. Amaducci, and P. Ouagne. 2019. Study of solutions to optimize the extraction of hemp fibers for composite materials. *SN Applied Sciences* 1 (10):1293.

Griffith, A. A., and G. I. Taylor. 1921. VI. the phenomena of rupture and flow in solids. *Philosophical Transactions of the Royal Society of London. Series A, Containing Papers of a Mathematical or Physical Character* 221 (582–593):163–98.

Hall, J., S. P. Bhattarai, and D. J. Midmore. 2014. The effects of photoperiod on phenological development and yields of industrial hemp. *Journal of Natural Fibers* 11:87–106.

Horne, M. R. L. 2020. Bast fibres: Hemp cultivation and production. In *Handbook of Natural Fibres*, ed. R. M. Kozłowski and M. Mackiewicz – Talarczyk, Vol. 1, 2nd ed ed., 163–96. Cambridge, MA: Elsevier.

Lefeuvre, A., A. Bourmaud, C. Morvan, and C. Baley. 2014. Elementary flax fiber tensile properties: Correlation between stress–strain behaviour and fiber composition. *Industrial Crops and Products* 52:762–69.

Liu, M., A. Baum, J. Odermatt, J. Berger, L. Yu, B. Zeuner, A. Thygesen, J. Holck, and A. S. Meyer. 2017. Oxidation of lignin in hemp fibers by laccase: effects on mechanical properties of hemp fibers and unidirectional fiber/epoxy composites. *Composites. Part A, Applied Science and Manufacturing* 95:377–87.

Liu, M., D. Fernando, G. Daniel, B. Madsen, A. S. Meyer, M. T. Ale, and A. Thygesen. 2015. Effect of harvest time and field retting duration on the chemical composition, morphology and mechanical properties of hemp fibers. *Industrial Crops and Products* 69:29–39.

Madsen, B., P. Hoffmeyer, and H. Lilholt. 2007. Hemp yarn reinforced composites – II. Tensile properties. *Composites. Part A, Applied Science and Manufacturing* 38 (10):2204–15.

Marrot, L., A. Bourmaud, P. Bono, and C. Baley. 2014. Multi-scale study of the adhesion between flax fibers and biobased thermoset matrices. *Materials & Design (1980-2015)* 62:47–56.

Marrot, L., A. Lefeuvre, B. Pontoire, A. Bourmaud, and C. Baley. 2013. Analysis of the hemp fiber mechanical properties and their scattering (Fedora 17). *Industrial Crops and Products* 51:317–27.

Müssig, J., S. Amaducci, A. Bourmaud, J. Beaugrand, and D. U. Shah. 2020. Transdisciplinary top-down review of hemp fiber composites: From an advanced product design to crop variety selection. *Composites Part C: Open Access* 2:100010.

Pasila, A. 2000. The Effect of Frost on Fiber Plants and Their Processing. *Molecular Crystals and Liquid Crystals Science and Technology. Section A. Molecular Crystals and Liquid Crystals* 353 (1):11–22.

Pickering, K. L., and M. G. Aruan Efendy. 2016. Preparation and mechanical properties of novel bio-composite made of dynamically sheet formed discontinuous harakeke and hemp fiber mat reinforced PLA composites for structural applications. *Industrial Crops and Products* 84:139–50.

Ranalli, P., and G. Venturi. 2004. Hemp as a raw material for industrial applications. *Euphytica* 140 (1):1–6.

Réquilé, S., A. Le Duigou, A. Bourmaud, and C. Baley. 2018. Peeling experiments for hemp retting characterization targeting biocomposites. *Industrial Crops and Products* 123:573–80.

Romhány, G., J. Karger-Kocsis, and T. Czigány. 2003. Tensile fracture and failure behavior of technical flax fibers. *Journal of Applied Polymer Science* 90 (13):3638–45.